Nucleation and growth of cholesteric fingers under electric field

P. Ribiere, P. Oswald

Classification
Physics Abstracts
61.30G — 61.30J

Nucleation and growth of cholesteric fingers under electric field

P. Ribiere and P. Oswald

Ecole Normale Supérieure de Lyon, Laboratoire de Physique, 46 Allée d'Italie, 69364 Lyon Cedex 07, France

(*Received on December 7, 1989, accepted in final form in February 26, 1990*)

Résumé. — Nous avons étudié le comportement d'un cristal liquide cholestérique placé entre deux plaques avec un ancrage homéotrope et en présence d'un champ électrique. En changeant les deux paramètres de contrôle, à savoir l'épaisseur de l'échantillon et l'amplitude du champ électrique, nous avons pu caractériser différents types de solutions : une phase nématique (cholestérique « déroulé »), des doigts isolés doublement torsadés, un réseau périodique de doigts arrangés côte à côte et une configuration transitoire simplement torsadée et invariante par translation. En incluant la contribution du champ électrique aux calculs de la référence [3], nous avons calculé un diagramme de phase théorique qui est en bon accord avec les données expérimentales. Il est essentiel, pour expliquer nos observations, de tenir compte de l'anisotropie des constantes élastiques.

Abstract. — We have studied the behavior of a cholesteric liquid crystal sandwiched between two plates, with homeotropic anchoring, in the presence of an electric field. By changing two control parameters, namely the sample thickness and the electric field magnitude, we were able to characterize different types of solutions : a nematic phase (unwound cholesteric), isolated doubly twisted fingers, a periodic pattern of fingers arranged side by side, and a transient singly twisted translationally invariant configuration. Including the electric field contribution to the calculations of reference [3], we have computed a theoretical phase diagram that agrees well with the experimental data. The consideration of anisotropic elasticity in our calculations was essential in explaining our observations.

1. Introduction.

A cholesteric phase is a nematic liquid that is twisted in a single direction. This structure is characterized by its pitch « p », i.e. the distance over which the director **n** (the unit vector parallel to the molecule) rotates of 2 π. A convenient way to obtain a large-pitch cholesteric is to dissolve a chiral molecule in a nematic liquid. For small concentrations, the pitch is inversely proportional to the concentration.

Cholesteric textures and associated topological defects have already been extensively studied, particularly in thick samples [1]. In this case, the influence of the boundary conditions can be disregarded.

The situation is very different in a confined geometry. In particular, when the anchoring on the surfaces limiting the sample is homeotropic (molecules perpendicular to the surface), the resulting frustration can completely unwind the cholesteric. This nematic-cholesteric transition has been described by several authors [2]. Recently, we have shown that elastic anisotropy implies that it is a first order transition [3]. Note that the control parameter of this unwinding transition is not the temperature but rather the dimensionless confinement ratio

$$C = d/p \tag{1}$$

where d is the thickness sample and p the natural cholesteric pitch.

There are two cases :

— $C > C_c \approx 1$, and the chiral structure can develop either as isolated fingers or as a periodic pattern,

— $C < C_c$, and the homeotropic nematic phase alone is stable.

It is also well known that another way to unwind a cholesteric structure is to apply an electric field. If the dielectric anisotropy of the molecule is positive it will tend to align along the field. By applying a large-enough electric field perpendicular to the helical axis, it is possible to unwind the cholesteric structure into a nematic phase [4].

In this article, we describe the behavior of a cholesteric phase submitted to both plate confinement and an electric field E. We show that in the (E, C) parameter plane, there are three different types of solutions : nematic and double twisted fingers, which can be either isolated or arranged into a periodic pattern (the so-called « fingerprint » texture).

We determine this phase diagram experimentally and then extend the theoretical model of reference [3] to the case of an applied electric field.

The plan of the body of the article is as follows : in section 2 we describe the topology of a finite-length finger. In particular, we show that its two ends are topologically different. In section 3 we describe the experimental set up. In section 4 we establish the phase diagram. Section 5 is a theoretical extension of the model of reference [3] that allowed us to draw up a phase diagram in good agreement with the experimental data.

2. Topology of a finger of finite length.

2.1 DTC MODEL. — The model which we use in this article has been extensively described in reference [3]. A convenient way to visualize the topology of a finger is to consider its image onto the unit sphere S2. The principle of this mapping is recalled in figure 1. At the moment, the finger is assumed to be rectilinear and infinite along the x-axis. In this case the image of a straight line $z = z_0$ (parallel to the y-axis i.e. normal to the finger) is a circle passing through the north pole, parameterized by the angle $\alpha(z_0)$ between its axis and the N.S. axis of the sphere and whose the center lies on another circle tangent to the north pole (whence a double-twist configuration (D.T.C. in the following) energetically favorable [3]) (Fig. 2). To insure the homeotropic anchoring on the glass plates, we take

$$\alpha(z_0) = \alpha_0 \sin(\pi z/d) \qquad (0 \leqslant z \leqslant d)\,. \tag{2}$$

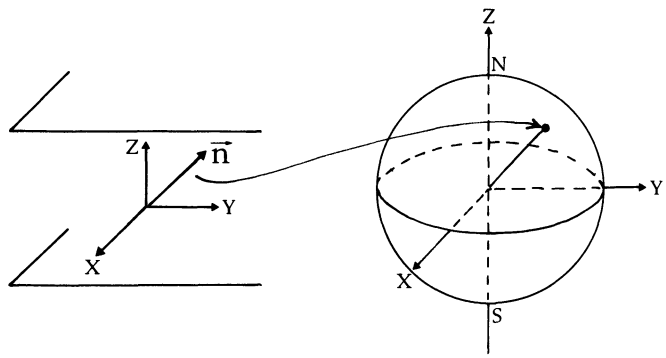

Fig. 1. — Representation on the sphere S2. As the director **n** changes orientation, it sweeps out a curve on S2. The same coordinate system is used in the real space and for the description of points on S2. By convention, the nematic phase is mapped to the north pole.

In this model, the angle α_0 plays the role of an order parameter for the transition : $\alpha_0 = 0$ corresponds to the nematic phase, $\alpha_0 \neq 0$ to a cholesteric finger. In figure 3, we have represented the director field for a finger of width λ. This molecular configuration is continuous and without any singularity, in contrast to the model proposed by Cladis and Kléman [5]. On the other hand, it is topologically equivalent to the model proposed by Press and Arrott [2].

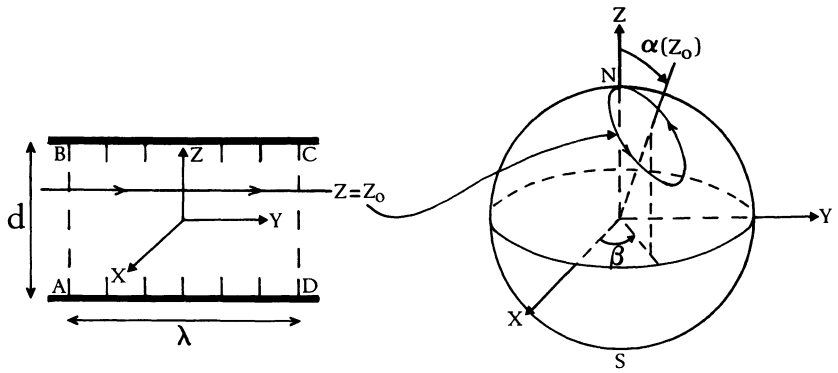

Fig. 2. — Double twisted finger of width λ. On the contour ABCD the director is parallel to the z-axis in order to insure the homeotropic anchoring on the glass plates and the matching with the outer nematic phase. The image of a line $z = z_0$ (parallel to the y-axis) onto the sphere is a circle of angle $\alpha(z_0)$ and passing through the north pole. The angle β is given by $\cos \beta = (\tan \alpha/2)/(\tan \alpha_0/2)$.

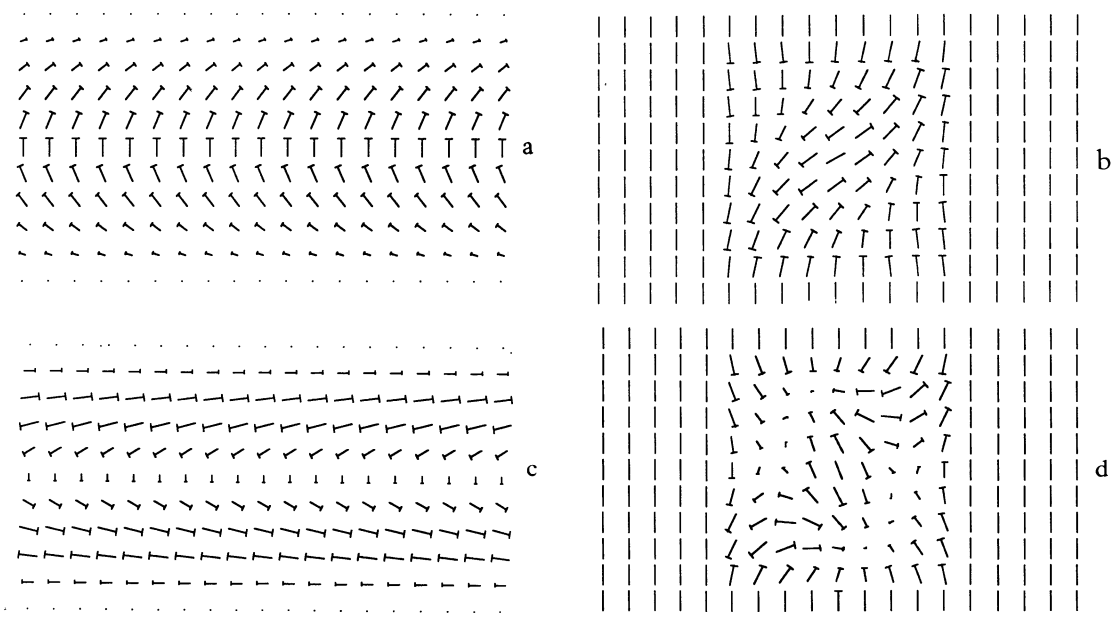

Fig. 3. — Director-field representation in a D.T. finger. A nail represents a molecule making an angle κ with the plane of the figure ; its length is proportional to $\cos \kappa$; the head of the nail is behind the plane of the figure and the tip is pointed on the observer : a) section by the median plane $z = d/2$, $\alpha_0 = 30°$; b) section by a plane perpendicular to the finger axis, $\alpha_0 = 30°$; c, d) *idem*, $\alpha_0 = 80°$. This molecular configuration resembles very closely the one described by Press and Arrott (Fig. 7 of Ref. [2d]).

2.2 TOPOLOGY OF A FINGER TIP. — A finger is never infinite. One possibility is that it may end at the sample edge. It may also form a loop (Fig. 4a) or a segment of finite length (Fig. 4b, c). In the last case two configurations are possible experimentally : either the two ends of the fingers are identical and there is always a defect inside the finger (Fig. 4b) [10] or there is no defect and the two ends of the finger are not the same, one end being sharper than the other (Fig. 4c).

To construct the topology of the finger ends without introducing singularities in the director field, it is sufficient to decrease continuously α_0 to zero at each end over a distance roughly equal to the finger width. Because the finger is not symmetrical with respect to a plane perpendicular to its axis (no mirror symmetry in a cholesteric), the ends are not identical. On

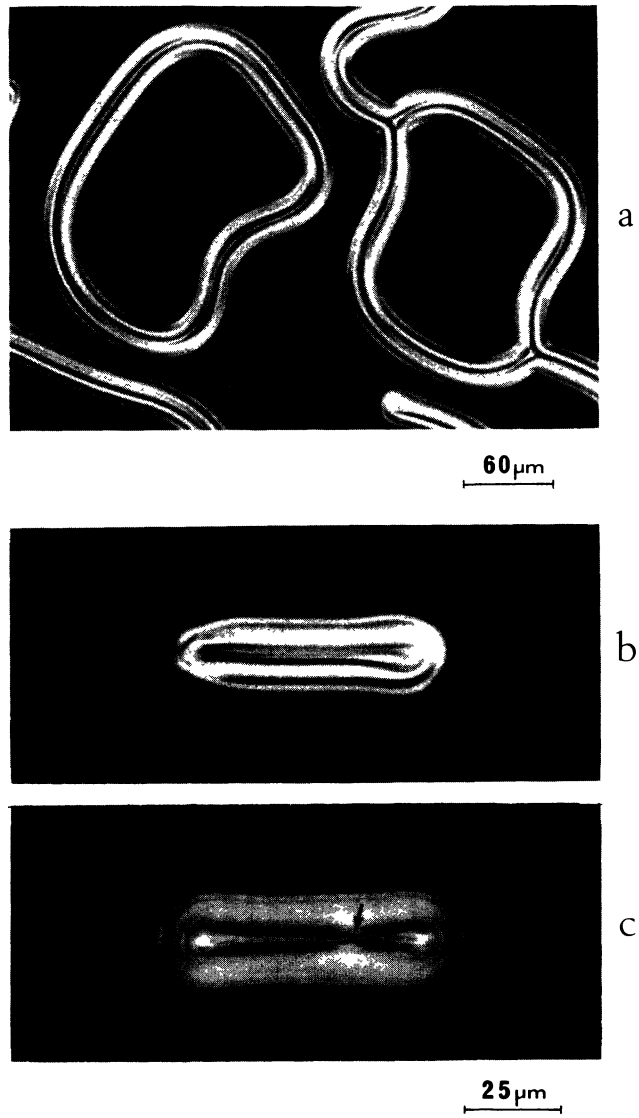

Fig. 4. — a) Finger forming a closed loop. b) Finger of finite length without any topological singularity. Note that one of its ends is charper than the other. c) Finger of finite length with two rounded, identical ends. The arrow indicates the presence of a $S = 1$ disclination normal to the glass plates.

the other hand, a calculation of **n** · **curl n** shows that at one of the ends the twist has everywhere the same sign as the spontaneous twist of the free cholesteric. At the other end, by contrast, the twist changes sign (Fig. 5a). We shall call the first one « normal tip » (or « + » tip) and the other « abnormal tip » (or « – » tip). When the two ends are identical, there is always a line defect (here a $S = 1$ disclination) joining the two glass plates in the bulk of the finger. This is shown in figure 5b. It is easy to see experimentally that the fracture of a finger (by applying an electric field, see below) leads to two ends of opposite signs. Conversely, two ends of opposite signs collapse together (Fig. 6) while two ends of the same sign repel and remain separated by a nematic slice. On the other hand, an abnormal tip can collapse with the side of a finger and form a T-like sidebranching (Fig. 7). On the contrary a normal tip is repelled by the side of a finger : the connection is impossible. This is explained in figure 8. This property allows us to characterize experimentally the two tip types. Thus the abnormal tips are sharper while the normal ones are rounded.

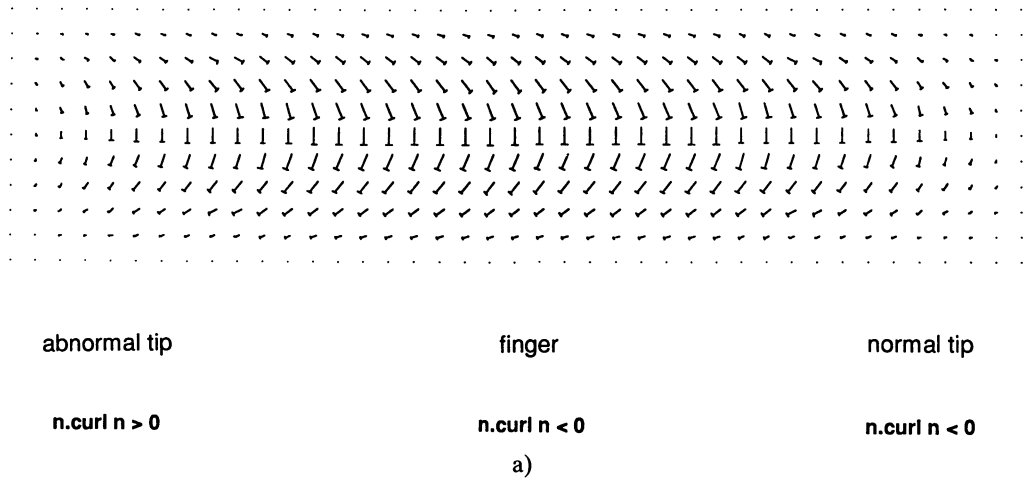

a)

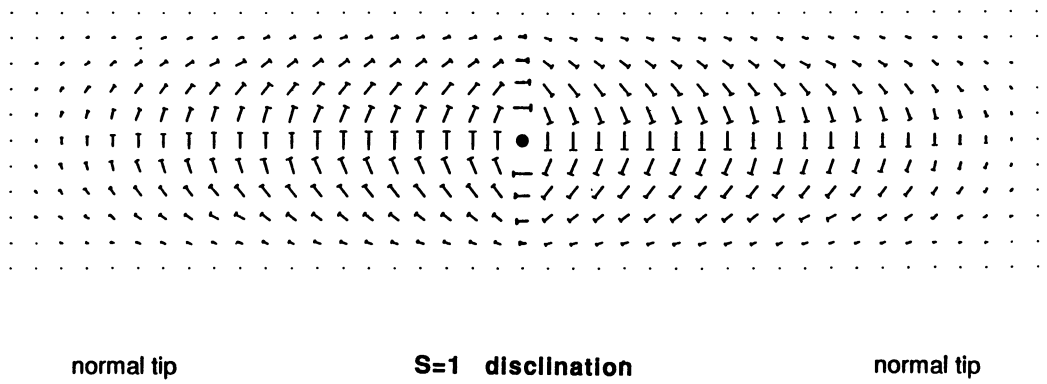

b)

Fig. 5. — a) Director-field representation in the two ends of a finger of finite length and in the median plane $z = 0$ ($\alpha_0 = 30°$). Calculation of **n** · **curl n** along the x-axis shows that, in one end, the twist is everywhere of the same sign as the spontaneous twist of the free cholesteric (normal end) while in the other, the twist changes sign (abnormal tip). b) Director-field representation when the two ends are identical (normal tips). A $S = 1$ disclination appears in the bulk of the finger.

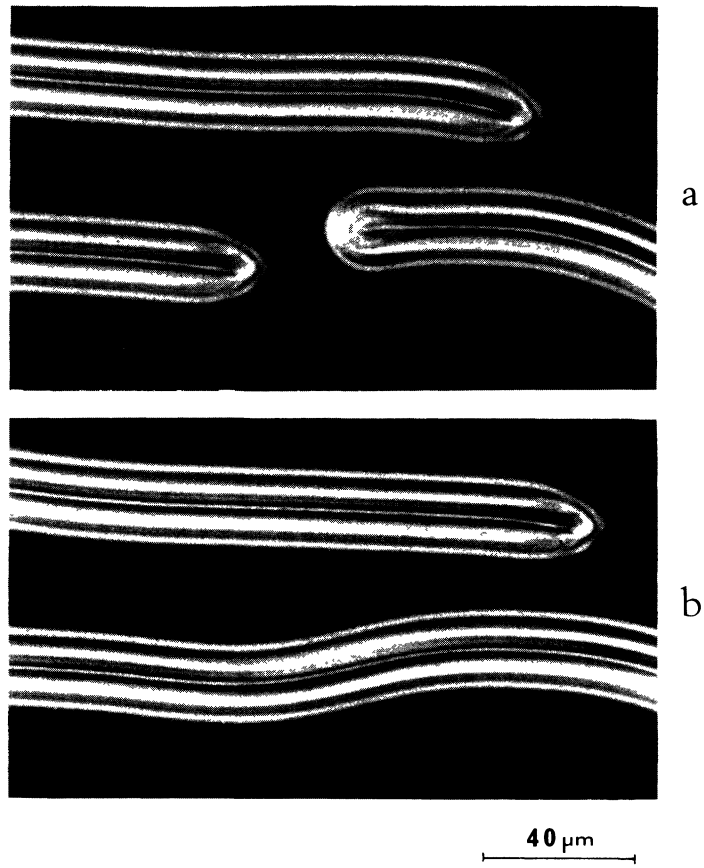

Fig. 6. — Fusion of an abnormal finger tip with a normal one ($C = 1.92$, $V = 4.8$ V) : a) just before connection ; b) after connection.

convective instabilities) until the cholesteric structure completely disappears so that the nematic phase is the only stable phase. Then we decrease abruptly the voltage down to the desired value. If a cholesteric texture appears it will be necessarily stable, the nematic phase being either metastable or unstable. By increasing again slowly the voltage, it is possible to determine the voltage at which this solution becomes metastable and then unstable. In this

3. Experimental set up.

The chosen materials are the eutectic nematic mixture ZLI 2452 (Merck) and the chiral molecule ZLI 811 (Merck). The concentrations are respectively 99.396 % and 0.604 % ww which corresponds to a cholesteric pitch close to 16.7 μm at room temperature (20 °C) (from Merck data). The mixture is placed between two conducting glass plates. The plates are coated with the silane ZLI 3124 (Merck) to orient the molecules perpendicular to the plates (homeotropic anchoring). The slides are fixed to two metallic holders coupled together *via* three differential screws. The thickness of the sample can be changed continuously from zero to 500 μm with an accuray of 0.1 μm. The thickness variations are measured using a LVTD-type transducer (Schaevitz) with an accuracy of ± 0.05 μm. A He-Ne laser is used to adjust

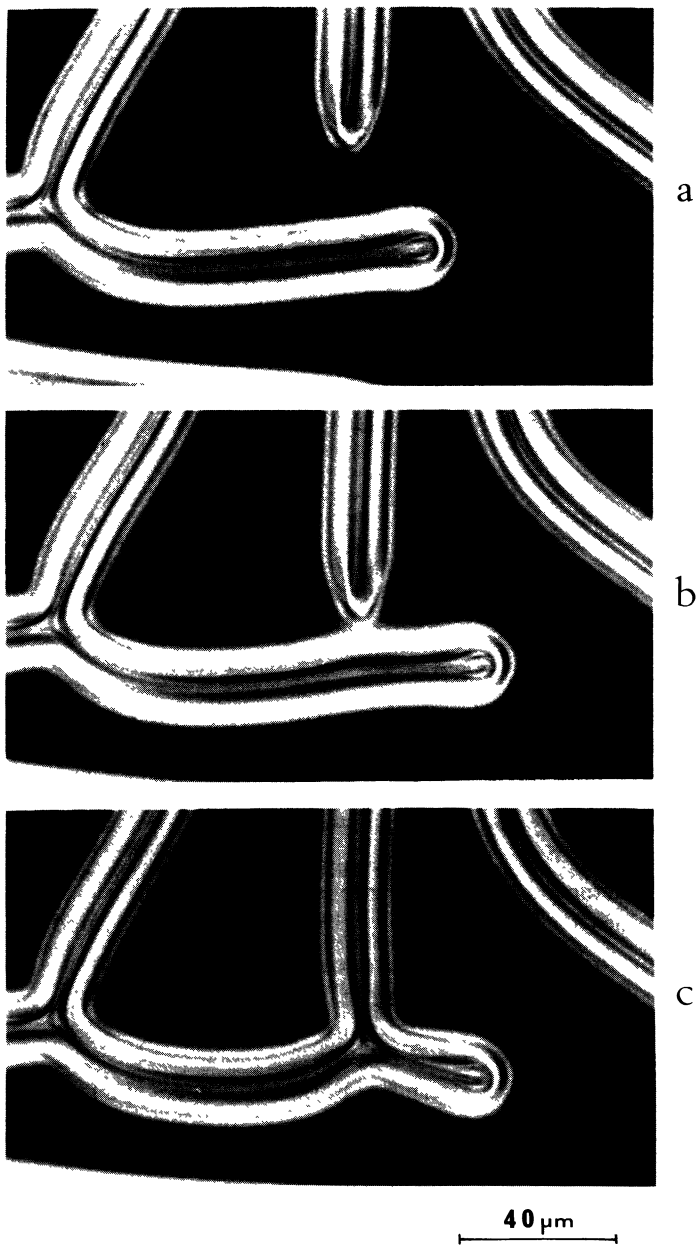

Fig. 7. — Junction of an abnormal finger tip with the side of an other finger ($C = 1.92$, $V = 4.8$ V) : a) just before connection ; b) after connection. A T-like sidebranching is formed.

the parallelism between the two plates to about $\pm 10^{-4}$ rd. Observations are made through a polarizing microscope Leitz between crossed polarizers.

4. Experimental phase diagram.

In order to establish the phase diagram, we adopted the following procedure : for a given thickness d, we increase the high-frequency applied voltage V (1 kHz in order to avoid

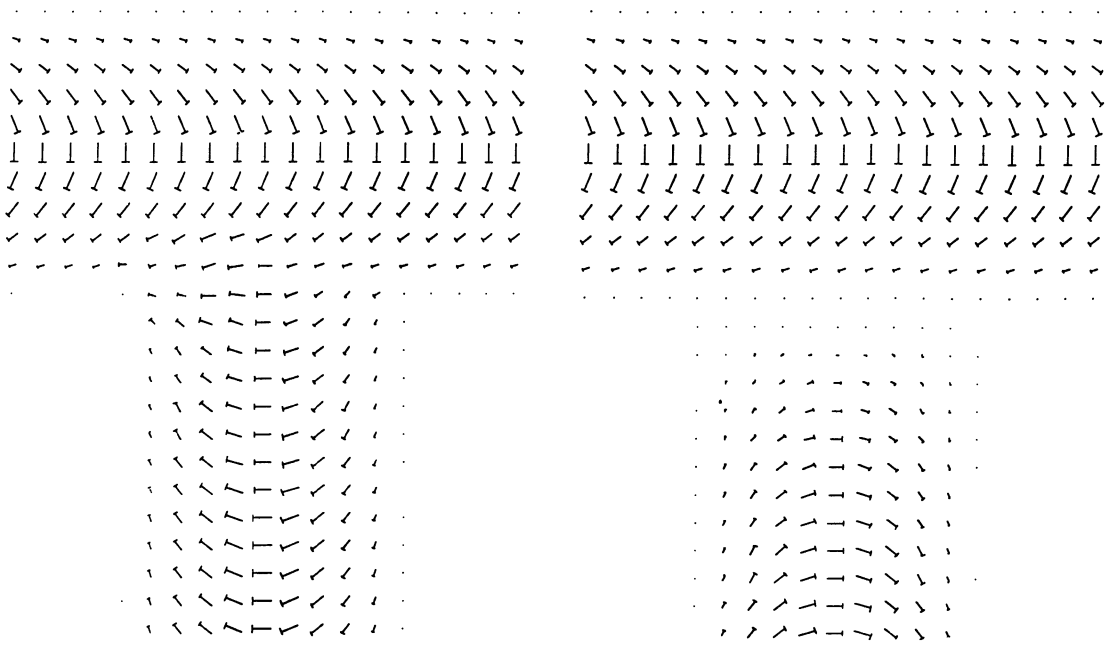

Fig. 8. — Director-field in the median plane ($z = 0$)($\alpha_0 = 30°$). a) T-like sidebranching formed after connection of an abnormal tip with the side of a finger ; b) because the twist is of the same sign in a normal tip and in the side of a finger, the connection is impossible and it remains a nematic slice between them.

way, it is possible to determine an unambiguous phase diagram. Five regions can be delimited according to the values of C and V. They correspond to three fundamental solutions :

— the first one is the homeotropic nematic phase (N) which is uniformly dark between crossed polarizers ;

— the second one corresponds to the isolated fingers (IF). Their width is well defined and they grow only from their two ends (Fig. 9) ;

— the third one is a periodic pattern of cholesteric fingers (PP). For certain values of the parameters, the isolated fingers are unstable with respect to tip-splitting instability. Only a periodic pattern can develop which fills up the space (Fig. 10) and leads to the so-called « fingerprint » texture. Note that only the normal tips can split.

It is important to note that these two solutions (IF and PP) are not transient and do not change after growth. Thus they correspond to a minimum of the free energy.

Let us also mention a translationally invariant configuration (TIC) which is twisted only in the direction normal to the glass plates. This solution is unstable with respect to the periodic pattern of fingers and can be observed only transiently (Fig. 11) [12].

Going back to the phase diagram of figure 12, we observe that :

— in region I (at high voltage or very small thickness), the nematic is stable and the cholesteric is unstable ;

— in region II, the nematic is still stable while the isolated fingers are metastable : they disappear from their ends without changing width. Finger-width measurements *versus* electric field are reported in figure 13a. On the line separating regions I and II, the fingers are

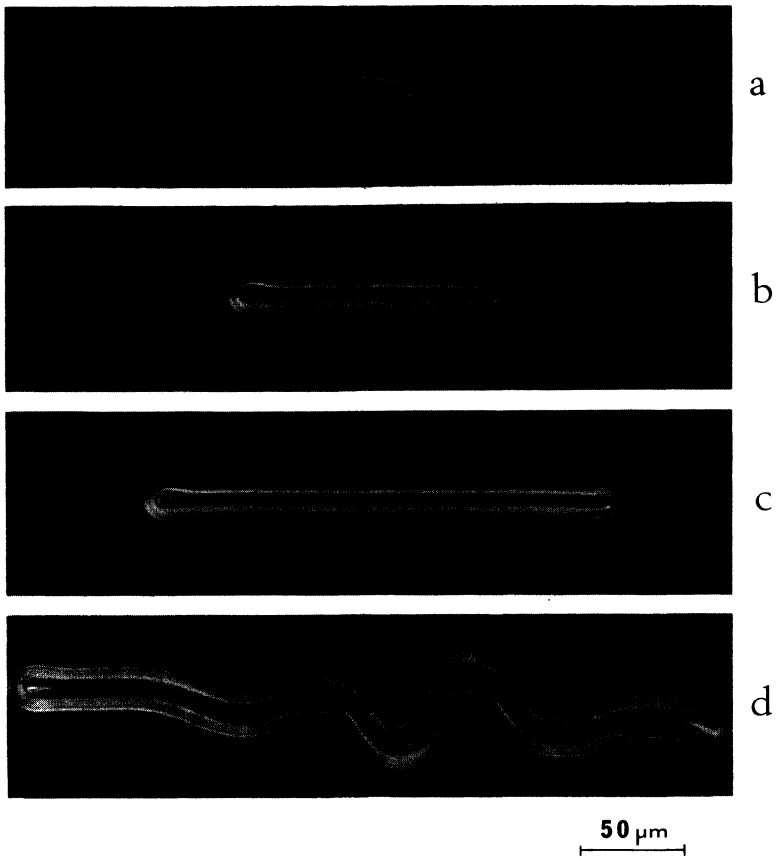

Fig. 9. — Growth of an isolated finger. a, b, c) Near the critical line (line 2 in the phase diagram), the finger grows very slowly and remains rectilinear : $C = 1.92$ and $V = 4.95$ V. d) When we decrease the voltage, the finger undulates spontaneously (explanation given in Appendix II) : $C = 1.92$ and $V = 4.30$ V.

unstable : they break up spontaneously in numerous places before disappearing in a few tenths of a second ;

— in region III, the nematic is metastable. The isolated fingers are stable and lengthen from their ends. They usually nucleate from dust particles which are always present in the samples, showing it is indeed a first order transition. Note that on the line dividing regions II and III, the two phases have the same free energy so that finger tips are motionless. As in the preceding region, it is possible to measure the finger width as a function of the electric field (Fig. 13). Note a tendancy of the fingers to spontaneously undulate, especially near the region IV discussed below ;

— in region IV, the nematic is still metastable. The isolated finger solution is unstable with respect to tip-splitting instability and replaced by the periodic solution which thereby becomes the only stable solution ;

— in region V, the nematic is unstable. « Quenching » the sample from region I into this region leads to the spontaneous formation of the transient TIC configuration. This solution is unstable (perhaps metastable) and slowly relaxes towards a double twist periodic structure similar to the fingerprint texture (Fig. 11).

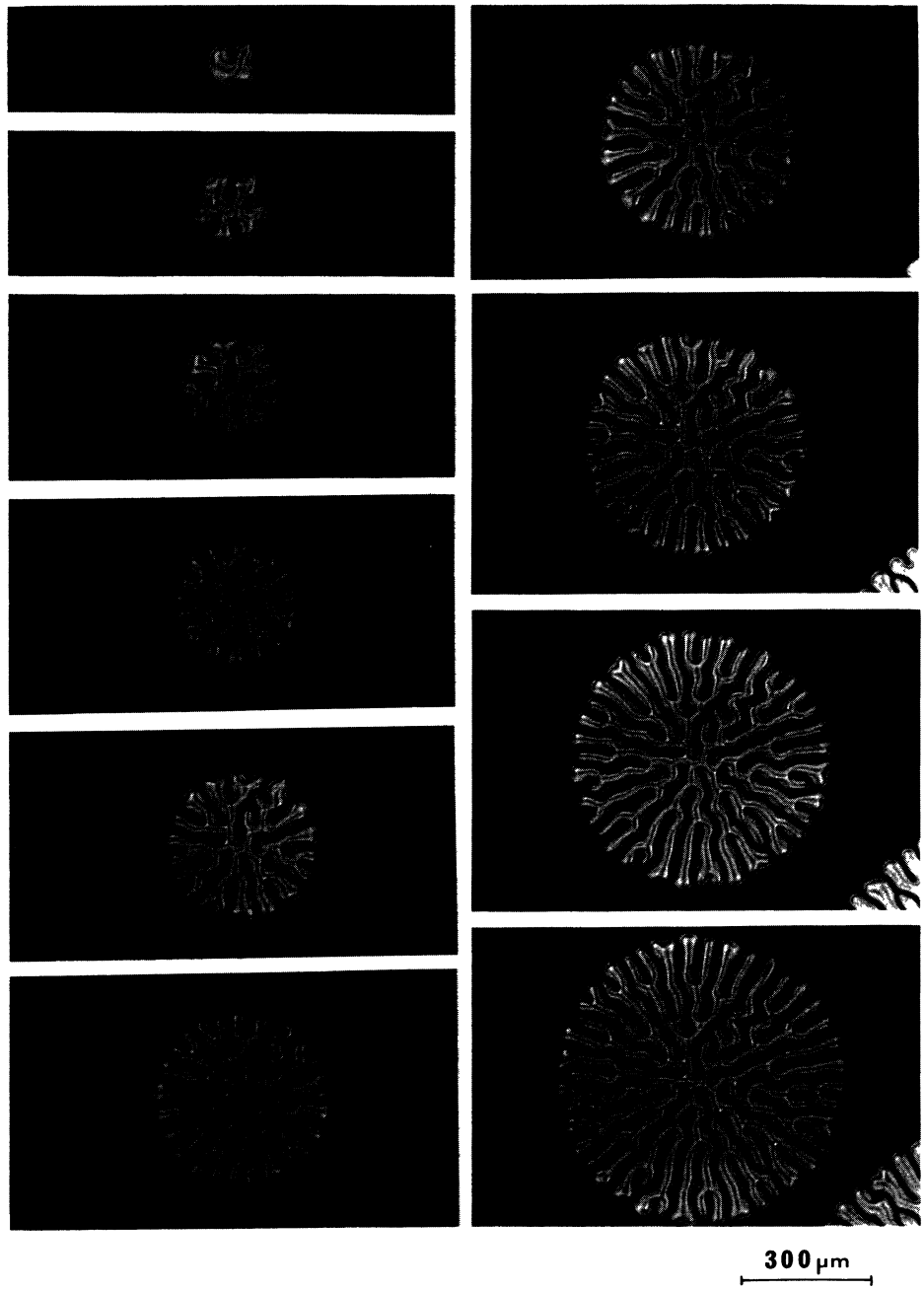

Fig. 10. — Growth of a periodic pattern of fingers ; $C = 1.23$ and $V = 1.18$ V. Successive photographs are at intervals of 4 s. Because of the circular geometry of the domain, splitting of the fingers is necessary to insure a constant mean wavelength. Note that this process leads to numerous edge dislocations in the finger pattern. Note also that normal tips split alone, and that the original abnormal tip remains unchanged during the growth and well visible on the pictures (the arrow indicates the abnormal tip).

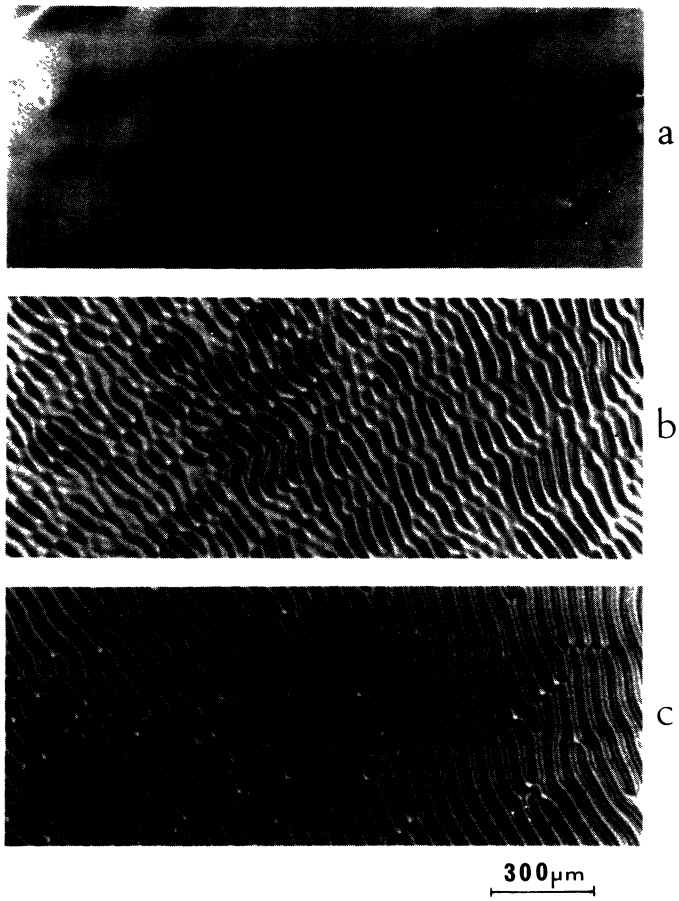

Fig. 11. — Spontaneous and homogeneous development of a T.I.C. configuration. $C = 1.92$ and $V = 0$. a) $t = 1$ s (after switching off the voltage) ; b) $t = 3$ s ; c) $t = 2$ min.

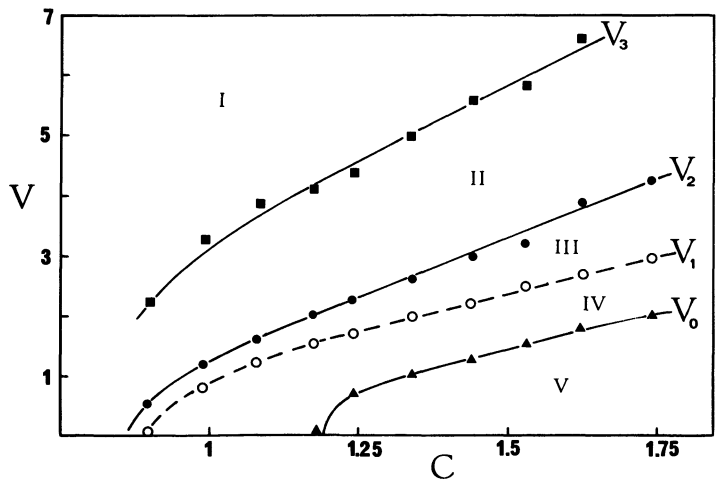

Fig. 12. — Experimental phase diagram. I) nematic phase ; II) metastable isolated fingers : they disappear from their ends but their width is well defined ; III) stable isolated fingers : they lengthen from their ends ; IV) periodic pattern ; V) transient translationally invariant configuration.

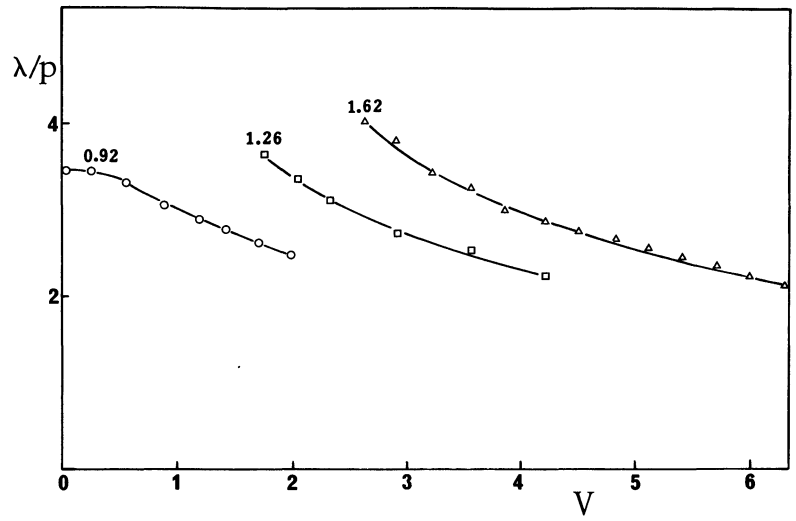

Fig. 13. — Finger width (in units of p) *versus* the voltage (in volt) for various values of the confinement ratio C. The width measurement is not precise (+ 15 %) because it depends upon the focusing and the optical conditions. Our measurements have been made between crossed polarizers and by focusing in the middle of the sample.

We conclude this section by noting that line 2 in this phase diagram is the critical line ($C = C_c(V)$) for coexistence between the two phases. Line 3 is the spinodal line above which the cholesteric isolated fingers are unstable, and line 0 the spinodal line of the nematic below which the TIC configuration spontaneously develops. Finally, line 1 is unusual : above it, isolated fingers grow, while below, only a periodic pattern develops.

5. Theoretical model.

In this section, we adopt the calculations of reference [3a] to include electric field effects. The basic geometrical model is the DTC model described in section 2. As in reference [3a], we assume that the trajectories of the director on the sphere are circular and we minimize the energy with respect to the width λ of the finger and its angle α_0. We recall that the free energy per unit volume of a cholesteric phase is (in S.I. units) [6] :

$$f = K_1/2(\text{div}\,\mathbf{n})^2 + K_2/2(\mathbf{n}\cdot\text{curl}\,\mathbf{n} + q)^2 + K_3/2(\mathbf{n}\times\text{curl}\,\mathbf{n})^2 - (\varepsilon_a\,\varepsilon_0/2)(\mathbf{E}\cdot\mathbf{n})^2 \quad (3)$$

where the K_i's ($i = 1, 2, 3$) are the elastic constants for, respectively, splay, twist, and bend deformations and $q = 2\pi/p$. The last term is the electric-field contribution. In the following, we shall define the energy of the homeotropic nematic state to be zero. We also assume, for the sake of simplicity, that E is constant and the applied voltage is given by $V = Ed$.

A straightforward calculation gives the energy F of a finger per unit length :

$$F(\lambda, \alpha_0)/K_2 = (1/K_2)\iint f\,\mathrm{d}y\,\mathrm{d}z = 2\pi kJ/q + 2\pi q(L + M/C + f(E))/k - 4\pi CI \quad (4)$$

with,

$$f(E) = \varepsilon_a\,\varepsilon_0\,E^2\,CN/K_2\,q^2 \quad \text{and} \quad k = 2\pi/\lambda\,. \quad (5)$$

The terms I, J, L, M, N are sums of integrals I_i depending upon α_0 (see Appendix I) :

$$I = I_{12}$$
$$J = K_{12}(I_1 + I_4) + I_2 + I_5 + K_{32}(I_3 + I_6)$$
$$L = I_{13}$$
$$M = K_{12} I_7 + I_8 + K_{32} I_9 + I_{10} + K_{32} I_{11}$$
$$N = I_{14}$$

with $K_{32} = K_3/K_2$ and $K_{12} = K_1/K_2$. It can be easily checked that :

$$\text{for} \qquad 0 < \alpha_0 < \pi/2\,, \quad I > 0\,, \quad J > 0\,, \quad L < 0\,, \quad M > 0\,, \quad N > 0\,. \tag{6}$$

Let us first consider an isolated finger (a case that was not considered in Ref. [3]). Minimization with respect to k (or λ) leads to the finger width :

$$\lambda = p\sqrt{CJ/(L + M/C + f(E))}\,. \tag{7}$$

The corresponding energy is after substitution into equation (4) :

$$F_{\text{I.F.}}(\alpha_0)/K_2 = 4\pi\sqrt{CJ(L + M/C + f(E))} - 4\pi CI\,. \tag{8}$$

Because of the inequalities noted in equation (6), $L + M/C + f(E)$ may vanish and become negative for certain values of the parameters E, C and α_0 : in such cases, the isolated finger is not a solution (its width becomes infinite). This is in agreement with our experiment, which shows that isolated fingers do not always exist. We shall see later that for these values of the parameters there still exists a periodic solution. To push further our theoretical predictions, we need to minimize F with respect to α_0 which requires numerical calculations. In figure 14 we plot F (in units of K_2) for two particular values of $C = d/p$ and various values of the voltage V (in volt). Calculations have been made with $K_{12} = 1.78$, $K_{32} = 2.38$ and $\pi\sqrt{K_1/\varepsilon_a\,\varepsilon_0} = 1.91$ V (see below). We now discuss these two examples in greater detail.

In figure 14a, $C = 1.10$. The isolated finger exists for all electric field values. For $V > V_3 \approx 1.0$ V, the only minimum is $\alpha_0 = 0$: the nematic is stable, the cholesteric unstable. For $V_3 > V > V_2 \approx 0.62$ V, there are two minima in $\alpha_0 = 0$ and $\alpha_0 \neq 0$ near to $\pi/4$: the nematic is stable and the cholesteric isolated finger is metastable. If $V < V_2$, there are still two minima, but the cholesteric isolated finger is now stable while the nematic becomes metastable.

In figure 14b, $C = 1.16$. The discussion remains unchanged as along as $V > V^* \approx 0.45$. For this value of the field and below, a divergence of the finger width appears : the located finger solution vanishes to the benefit of the periodic solution that we discuss briefly below (see Ref. [3a] for more details).

Up to now, we have been interested only in localized solutions. It is also possible to consider periodic pattern of fingers arranged side by side. In this case the quantity to minimize is $F(\lambda, \alpha_0)/\lambda$ i.e. the energy per unit area of the pattern. A simple calculation gives (in units of $K_2 q$) :

$$F_{\text{P.P.}}(\alpha_0)/K_2 q = -CI^2/[J + L + M/C + f(E)] \tag{9}$$

for an optimal wavelength :

$$\lambda = pJ/I\,. \tag{10}$$

One sees immediately that λ is always defined and depends through α_0 upon the electric field, but not directly.

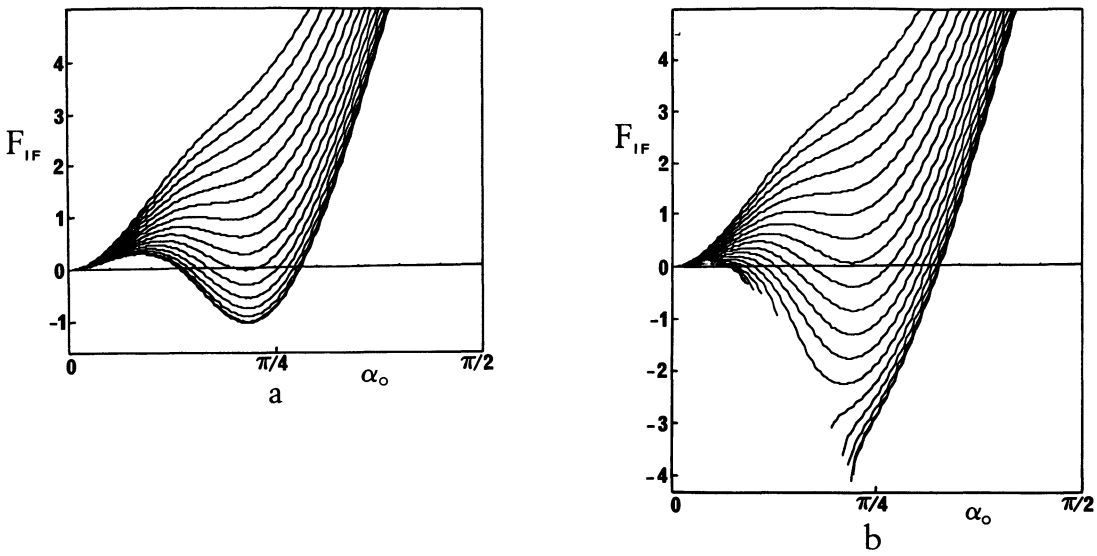

Fig. 14. — Free energy per unit length (in units of K_2) of an isolated finger as a function of the voltage. a) $C = 1.1$ and the voltage varies from 0 to 1.5 V by increment of 0.1 V ; b) $C = 1.16$ and the voltage varies from 0 to 1.7 V by increment of 0.1 V ; when V is lower than $V^* \approx 0.45$ V, the energy is no longer defined for all values of α_0 and the finger-width diverges.

Thus a periodic structure is expected (and indeed observed experimentally) for all values of the voltage lower than $V^*(C)$. As a matter of fact we have never observed the divergence of the width of an isolated finger but only an increase in width (see Fig. 13) and line 1 in the experimental phase diagram does not exactly coincide with $V^*(C)$. To determine analytically the value of the field $V_1(C)$ below which the periodic solution develops (with necessarily $V_1(C) > V^*(C)$), we must analyze the tip-stability of a growing isolated finger. This is a difficult calculation that we have not done. Nevertheless, the experiment shows that the tip-splitting instability occurs as soon as the width $\lambda_{\text{I.F.}}$ of an isolated finger is roughly equal to 1.4 $\lambda_{\text{P.P.}}$ where $\lambda_{\text{P.P.}}$ is the wavelength of the corresponding periodic solution [9]. This experimental crude criterion, which results from a dynamical process, allows to estimate a theoretical value for $V_1(C)$ (line 1 in the phase diagram).

Finally we calculate the spinodal line corresponding to the nematic phase (line 0 in the phase diagram). It is the curve below which the T.I.C. configuration develops spontaneously [7]. In reference [3], we showed that this occurs at zero electric field when $C \geqslant K_{32}/2$. This calculation can be easily extended to the case of an applied electric field. It yields :

$$V_0(C)/(\pi \sqrt{K_1/\varepsilon_a \varepsilon_0}) = (2/\sqrt{K_{12}}) \sqrt{(C - K_{32}/2)}\,. \tag{11}$$

In figure 15, we plot V_0 (experimental) as a function of $\sqrt{(C - K_{32}/2)}$ and find a good linear dependance. From these data, we obtain $K_{32} \approx 2.38$ and $\pi/\sqrt{K_1/\varepsilon_a \varepsilon_0} \approx 1.91$ V knowing that $K_{12} \approx 1.78$ (from Merck data).

In conclusion, we have all the theoretical tools we need to predict the phase diagram, represented in figure 16. In spite of a few shifts of the calculated curves with respect to the experimental ones (certainly due to the crude assumption that director trajectories are always circles, even in the presence of an electric field, and to the uncertainty about the K_{ij} values), the theoretical diagram closely resembles the experimental one of figure 12. Also,

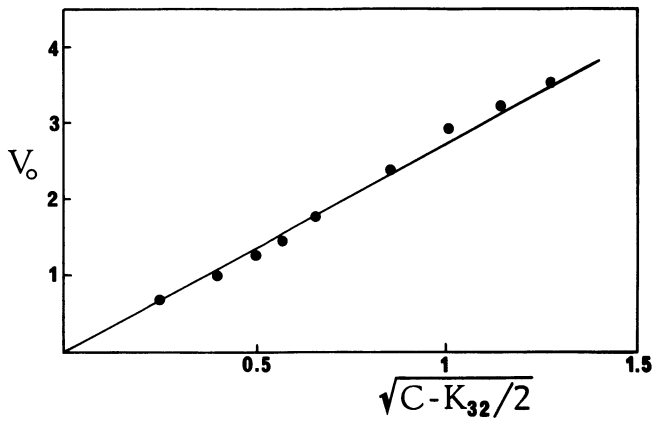

Fig. 15. — V_0 (experimental) *versus* $\sqrt{C - K_{32}/2}$ with $K_{32}/2 = 1.19$.

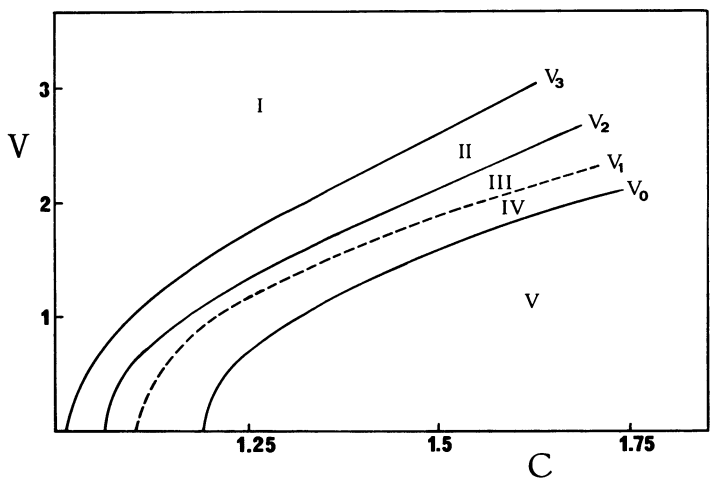

Fig. 16. — Theoretical phase diagram.

we show in figure 17 theoretical predictions for the width λ of an isolated finger as a function of the electric field. Here again, a good qualitative agreement is found with the experimental data (Fig. 13). All these results fully confirm the validity of our geometrical approach of this unwinding transition. Once again, note that these calculations took into account anisotropic elasticity (whence our approximations) ; otherwise, it would be impossible to explain the first-order character of this transition and most of our observations. Finally we give in appendix II a rough calculation which accounts qualitatively for the undulation instability observed in isolated fingers.

In the future, it would be interesting to extend this work to the dynamics of the nematic-cholesteric interfaces that we previously observed in the presence of a temperature gradient [8].

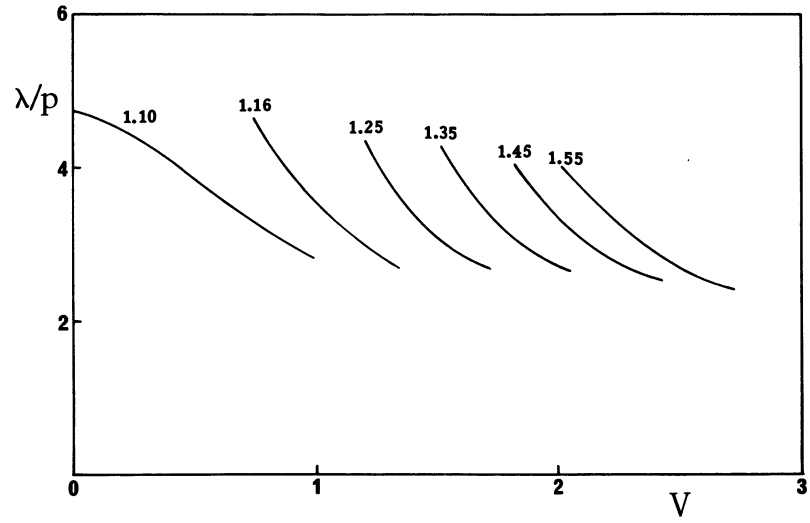

Fig. 17. — Finger-width *versus* the applied voltage (in volt) for various values of the confinement ratio C : theoretical prediction based on equation (7).

Acknowledgments.

We thank F. Lequeux and J. Bechhoefer for useful discussions. This work was supported by D.R.E.T. contract No 88/1365.

Appendix I

$$I_1 = \int_0^{\pi/2} (\cos^2 \alpha - \cos^4 \alpha)\, dZ$$

$$I_2 = \int_0^{\pi/2} (2 - 6\cos^2 \alpha + 7\cos^4 \alpha - 3\cos^6 \alpha)\, dZ$$

$$I_3 = \int_0^{\pi/2} (3\cos^2 \alpha - 6\cos^4 \alpha + 3\cos^6 \alpha)\, dZ$$

$$I_4 = \int_0^{\pi/2} \sin^2 \beta \sin^4 \alpha\, dZ$$

$$I_5 = \int_0^{\pi/2} \sin^2 \beta (-2 + 7\cos^2 \alpha - 8\cos^4 \alpha + 3\cos^6 \alpha)\, dZ$$

$$I_6 = \int_0^{\pi/2} \sin^2 \beta (1 - 5\cos^2 \alpha + 7\cos^4 \alpha - 3\cos^6 \alpha)\, dZ$$

$$I_7 = \int_0^{\pi/2} 6\cos^2 \alpha \sin^2 \alpha\, \dot{\alpha}^2\, dZ$$

$$I_8 = \int_0^{\pi/2} \frac{5}{8} \sin^6 \alpha\, \dot{\alpha}^2\, dZ$$

$$I_9 = \int_0^{\pi/2} \frac{1}{8} \dot{\alpha}^2 (7 - 29\cos^2 \alpha + 33\cos^4 \alpha + 5\cos^6 \alpha)$$

$$I_{10} = \int_0^{\pi/2} \frac{1}{8} \dot{\beta}^2 (3 + 4\cos^2\alpha + 18\cos^4\alpha - 60\cos^6\alpha + 35\cos^8\alpha)\, dZ$$

$$I_{11} = \int_0^{\pi/2} \frac{1}{8} \dot{\beta}^2 (1 + 4\cos^2\alpha - 30\cos^4\alpha + 60\cos^6\alpha - 35\cos^8\alpha)\, dZ$$

$$I_{12} = \int_0^{\pi/2} 2\sin^3\alpha \cos\beta\, dZ$$

$$I_{13} = \int_0^{\pi/2} \dot{\beta} \sin^2\alpha (1 + 3\cos^2\alpha)\, dZ$$

$$I_{14} = \int_0^{\pi/2} (2 - 2\cos^4\alpha - \sin^4\alpha)\, dZ$$

with $Z = \frac{\pi z}{d}$, $\alpha = \alpha_0 \sin Z$

and $\cos\beta = \frac{\tan\alpha/2}{\tan\alpha_0/2}$ and $\cdot$ means $\frac{\partial}{\partial Z}$.

Appendix II.

Undulation instability of an isolated finger.

The experiment shows clearly that an isolated finger tends to undulate spontaneously with a wavelength that decreases with the electric field. This undulation results from a balance between the energy decrease due to the finger's larger area and the elastic energy increase due to its local bending. To derive this result, let a and Λ be the amplitude and wavelength of the undulation :

$$y = a \sin (2\pi x/\Lambda) \qquad a \ll \Lambda . \tag{12}$$

Calculation of the length increase per unit finger, length (along the x-axis) yields the free energy gained :

$$F_{\text{I.F.}}\, \pi^2 a^2/\Lambda^2 \tag{13}$$

where $F_{\text{I.F.}}$ is given by equation (8).

By analogy with rod elasticity, we assume that the bend energy of a finger is proportional to the square of its curvature $1/R$. Thus we write the curvature energy in the form :

$$CK\Sigma/R^2 = 8\pi^4 CK\Sigma a^2/\Lambda^4 \tag{14}$$

K is a Frank modulus, $\Sigma = \lambda d$ the area of a vertical section of the finger and C a numerical constant.

Adding the two terms, we get the free-energy variation :

$$\Delta F_{\text{I.F.}} = F_{\text{I.F.}}\, \pi^2 a^2/\Lambda^2 + 8\pi^4 CK\Sigma a^2/\Lambda^4 . \tag{15}$$

This quantity is minimized when

$$\Lambda = 4\pi \sqrt{CK\Sigma/(-F_{\text{I.F.}})} \tag{16}$$

corresponding to

$$\Delta F_{\text{I.F.}} = -(K/32\,C)(a^2/\Sigma)(F_{\text{I.F.}}/K)^2 < 0 . \tag{17}$$

We conclude that an isolated finger undulates spontaneously as soon as $F_{I.F.}$ is negative, that is in region III of the phase diagram. As one approaches the critical line 2, $F_{I.F.}$ goes to zero and Λ becomes infinite : close to this line the fingers must be almost rectilinear while undulations appear progressively as the electric field is decreased ($|F_{I.F.}|$ increases as E decreases). These theoretical predictions are in very good qualitative accord with our observations. Quantitative comparison with the experiment requires a calculation of the numerical constant C. This is a rather tedious calculation that we have not done.

References

[1] BOULIGAND Y., *J. Phys. France* **34** (1973) 603 ; **35** (1974) 959.

[2] For the experimental evidence of the unwinding transition induced by the plates confinement see :
a) BREHM, FINKELMANN H. and STEGEMEYER H., *Ber. Bunsenges. Phys. Chem.* **78** (1974) 883.
b) HARVEY T., *Mol. Cryst. Liq. Cryst.* **34** (1978) 224.
For a theoretical calculation in isotropic elasticity and observations under magnetic field see :
c) PRESS M. J. and ARROTT A. S., *J. Phys. France* **37** (1976) 387.
d) PRESS M. J. and ARROTT A. S., *Mol. Cryst. Liq. Cryst.* **37** (1976) 81.

[3a] LEQUEUX F., OSWALD P. and BECHHOEFER J., *Phys. Rev. A* **40** (1989) 3974.

[3b] LEQUEUX F., *J. Phys. France* **49** (1988) 967.

[4] DE GENNES P. G., *Solid State Commun.* **6** (1968) 163 ;
MEYER R. B., *Appl. Phys. Lett.* **14** (1969) 208.

[5] CLADIS P. E. and KLÉMAN M., *Mol. Cryst. Liq. Cryst.* **16** (1972) 1.

[6] DE GENNES P. G., The Physics of Liquids Crystals (Oxford University Press, Oxford) 1974.

[7] We showed in reference [3] that both the periodic solution and the T.I.C. configuration become unstable at the same critical parameters values. Thus, the selection between these two solutions is purely dynamical, the T.I.C. configuration having a greater growth rate than the periodic solution.

[8] OSWALD P. *et al., Phys. Rev. A* **36** (1987) 5832.

[9] It is possible to show that the critical line for both solutions, namely the isolated fingers and the periodic solution, is the same (line 2 in the phase diagram). The reason for which we did not observe the periodic solution in region III, but only the isolated fingers, is dynamical and related to the nucleation and growth processes. On the other hand, our static calculation shows that the isolated fingers can only be observed in a well defined region of the phase diagram, namely between the lines $V_2(C)$ and $V^*(C)$.

[10] Such a defect has been previously observed by several authors. See for instance :
a) KAWACHI M., KOGURE O., KATO Y., *Japan J. Appl. Phys.* **13** (1974) 1457 ;
b) BHIDE V. G., CHANDRA S., JAIN S. C., MEDHEKAR R. K., *J. Appl. Phys.* **47** (1976) 120 ;
c) AKAHANE T., TAKO T., *Mol. Cryst. Liq. Cryst.* **38** (1977) 251.